

MRI-PHY/P970922

September, 1997

hep-ph/9709392

# Filtering Out Signals of Gauge-Mediated Supersymmetry Breaking: Can We Always Eliminate Conventional Supersymmetric Effects ?

Biswarup Mukhopadhyaya<sup>1</sup> and Sourov Roy<sup>2</sup>*Mehta Research Institute, Chhatnag Road, Jhusi, Allahabad - 211 019, INDIA*

## ABSTRACT

We investigate the signal  $\gamma\gamma + \not{E}$  in a high-energy linear  $e^+e^-$  collider, with a view to differentiating between gauge-mediated supersymmetry breaking and the conventional supersymmetric models. *Prima facie*, there is considerable chance of confusion between the two scenarios if the assumption of gaugino mass unification is relaxed. We show that the use of polarized electron beams enables one to distinguish between the two schemes in most cases. There are some regions in the parameter space where this idea does not work, and we suggest some additional methods of distinction. We also perform an analysis of some signals in the gauge-mediated model, coming from the pair production of the second-lightest neutralino.

PACS NOS. : 12.60.Jv, 13.10.+q, 14.80.Ly

<sup>1</sup>E-mail : biswarup@mri.ernet.in<sup>2</sup>E-mail : sourov@mri.ernet.in

# 1 Introduction

The search for supersymmetry (SUSY) [1] is intimately connected with the issue of SUSY breaking, since the latter often dictates low-energy phenomenology, based on which search strategies are devised. In recent times, a lot of attention has been focused on theories where SUSY breaking is conveyed to the “visible” sector through the ordinary standard model (SM) gauge interactions. Obviously, one would like to know whether it is possible to distinguish between these SUSY breaking schemes and the more popular ones where gravitational interactions play the decisive role. From a phenomenological point of view, this boils down to a distinction between the experimental signals of the alternative scenarios.

In models with gauge-mediated SUSY breaking (GMSB) [2, 3, 4, 5, 6] the supersymmetric partner of the graviton, i.e., the gravitino ( $\tilde{G}$ ) is very light (practically massless compared to the electroweak scale) and is the lightest supersymmetric particle (LSP). The lightest standard model superpartner, which is the LSP in the scenario motivated by minimal supergravity (SUGRA), now becomes the next to lightest supersymmetric particle (NLSP). A natural consequence is that the NLSP can now decay into its supersymmetric partner and a gravitino. If the NLSP is a neutralino and decays inside the detector, then in collider searches one can see signatures of the type  $\gamma\gamma + \cancel{E}$ ,  $\gamma + \cancel{E}$  etc. [7, 8, 9, 10, 11], of which the first one is most promising and well studied. This has to be contrasted with the SUGRA-based schemes where the gravitino is as massive as the electroweak scale itself, and the LSP is stable.

A considerable amount of effort has been spent to ensure that the  $\gamma\gamma + \cancel{E}$  signal for GMSB rises above SM backgrounds [12]. It is, however, equally important to understand whether this signal can ever be mimicked in the conventional minimal SUSY models (henceforth to be described as the MSSM case in this paper), and to suggest effective methods of distinction in such cases.

In this paper, we confine ourselves to high-energy  $e^+e^-$  collision experiments. We argue

that the  $\gamma\gamma + \cancel{E}$  signals may come from the MSSM scenario as well, if we relax the condition of gaugino mass unification at an energy scale  $\sim 10^{16}$  GeV. In that case, as has already been shown in the literature [13], radiative decays of the second lightest neutralino ( $\tilde{\chi}_2^0$ ) into a photon and the LSP ( $\tilde{\chi}_1^0$ ) is dominant in certain regions of the parameter space. Pair-produced  $\tilde{\chi}_2^0$ 's may then give rise precisely to the type of signals mentioned above, sometimes with comparable strength. We suggest two ways of distinguishing the GMSB and MSSM cases, namely, (i) the use of polarized electron beams and (ii) the distributions in the total energy of the two emitted photons. And finally, we briefly study the signals coming from  $\tilde{\chi}_2^0$  pairs in the GMSB scheme.

The paper is organized as follows. In section 2, we give a brief description of the minimal model of gauge-mediated supersymmetry breaking. In section 3, we analyze and compare the two-photon signal both from GMSB and MSSM. Prospects of signals from  $\tilde{\chi}_2^0$  pairs in GMSB are discussed in section 4. Section 5 contains our conclusions.

## 2 The minimal GMSB model - a brief description

The minimal model of gauge-mediated supersymmetry breaking [14] requires a messenger sector consisting of vectorlike quark and lepton superfields which are coupled to a  $SU(3) \times SU(2) \times U(1)$  singlet superfield  $S$ , through the superpotential

$$W = \lambda S \bar{\Psi} \Psi. \quad (1)$$

The fields  $\Psi$  and  $\bar{\Psi}$  lie in a complete  $5 + \bar{5}$  representation of  $SU(5)$  in order to maintain gauge coupling unification.<sup>1</sup>

---

<sup>1</sup>Actually, up to four generations of  $5 + \bar{5}$  or one  $5 + \bar{5}$  and one  $10 + \bar{10}$  are allowed. We consider only one generation here.

The scalar ( $S$ ) and auxiliary ( $F_S$ ) components of  $S$  acquire vacuum expectation values (VEVs) through their interactions with the hidden sector where SUSY is broken dynamically. These VEVs induce masses for the messenger fields and lift the mass-degeneracy between the messenger fermions and sfermions. The breakdown of SUSY is communicated to the visible world radiatively via the SM gauge interactions. Thus, the observable gauginos and scalars acquire masses at the one-loop and two-loop levels, respectively.

The expressions for the masses of gaugino ( $M_{\frac{1}{2}}$ ) and scalars ( $M_0$ ) are

$$M_{\frac{1}{2}}(M) = N_m f_1 \left( \frac{\Lambda}{M} \right) \frac{\alpha_i(M)}{4\pi} \Lambda, \quad (2)$$

$$M_0^2(M) = 2 N_m f_2 \left( \frac{\Lambda}{M} \right) \sum_{i=1}^3 k_i C_i \left( \frac{\alpha_i(M)}{4\pi} \right)^2 \Lambda^2 \quad (3)$$

at the scale  $M$ , where  $M = \lambda \langle S \rangle$  and  $\Lambda = \frac{\langle F_S \rangle}{\langle S \rangle}$ .  $M$  determines the overall scale of the messenger sector;  $\Lambda$  controls particle-sparticle splitting in that sector as well as sparticle masses in the observable sector. The messenger scale threshold functions are given by

$$f_1(x) = \frac{1+x}{x^2} \ln(1+x) + (x \rightarrow -x) \quad (4)$$

$$f_2(x) = f_1(x) - \frac{2(1+x)}{x^2} \left[ \text{Li}_2 \left( \frac{x}{1+x} \right) - \frac{1}{4} \text{Li}_2 \left( \frac{2x}{1+x} \right) \right] + (x \rightarrow -x). \quad (5)$$

In Eq.(3),  $C_i = 0$  for all gauge singlets and is equal to  $\frac{4}{3}, \frac{3}{4}, \left( \frac{Y}{2} \right)^2$  for scalars belonging to the fundamental representations of  $SU(3)$ ,  $SU(2)$ , and  $U(1)$ , respectively.  $Y = 2(Q - T_3)$  is the usual weak hypercharge and  $k_i = 1, 1, \frac{5}{3}$  for these three groups (we do not use grand unification normalization for  $\alpha_1$ ).  $N_m$  is the number of messenger generations; in our case  $N_m = 1$ . We have taken into account the contributions from the usual D terms and the weak scale threshold corrections while evolving the sfermion masses from messenger( $M$ ) scale down to the electroweak scale. We do not consider the messenger scale threshold corrections because they are model dependent. Thus, MSSM phenomenology is determined

in terms of the parameters  $\Lambda$ ,  $x = \frac{\Lambda}{M}$ ,  $\tan\beta$  [the ratio of the two Higgs vacuum expectation values(VEVs)] and  $\mu$  (the Higgsino mass parameter).

### 3 Analysis of the two-photon signals

The two-photon signal may come from a GMSB scenario where the lightest neutralino ( $\tilde{\chi}_1^0$ ) is the NLSP. The production of a pair of such NLSPs, followed by each decaying to a photon and a gravitino, leads to the signal

$$e^+e^- \longrightarrow \tilde{\chi}_1^0\tilde{\chi}_1^0 \longrightarrow \gamma\gamma + \cancel{E}$$

Detailed calculations on this signal have been performed in many recent works in the contexts of the current hadronic [15] and  $e^+e^-$  colliders [16] as well as the proposed Next Linear Collider (NLC) [17]. By far the strongest limits on sparticle masses set so far from such signals are those imposed on the lightest chargino and neutralino by the D $\emptyset$  group [18]:  $m_{\tilde{\chi}^\pm} > 150$  GeV,  $m_{\tilde{\chi}_1^0} > 75$  GeV. We begin by reporting a repeat calculation for an  $e^+e^-$  collider at  $\sqrt{s} = 500$  GeV. The SM backgrounds have been removed here by using the following set of cuts:

1.  $|M_{inv} - M_Z| \geq 20$  GeV

2.  $(p_T)_\gamma \geq 20$  GeV

3.  $40^\circ < \theta_\gamma < 140^\circ$

where we define  $M_{inv}$  as:

$$M_{inv}^2 = (P_{e^-} + P_{e^+} - P_{\gamma_1} - P_{\gamma_2})^2 \quad (6)$$

The invariant mass cut eliminates the backgrounds from  $e^+e^- \longrightarrow Z\gamma\gamma$ , whereas the  $p_T$ -cuts take care of events such as  $e^+e^- \longrightarrow \nu\bar{\nu}\gamma\gamma$  through t-channel W exchange. Finally, selecting

highly central events by imposing a polar angle cut on each observed photon ensures that the photon is coming from the decay of a heavy particle. GMSB signals are found to survive these cuts to a large extent.

In Fig. 1, we plot the cross section of  $\gamma\gamma$  events as a function of  $\Lambda$  for a center-of-mass energy 500 GeV, for unpolarized, left-polarized, and right-polarized electron beams, the positrons being unpolarized in each case. Only representative combinations of  $\mu$  and  $\tan\beta$  is chosen for these graphs. As is clear from the previous sections, the masses of the superparticles increase with  $\Lambda$ ; therefore a lower limit on  $\Lambda$  can be inferred from the mass bounds on the charginos and neutralinos. Our numerical study extends from this lower limit to the kinematic limit of  $\tilde{\chi}_1^0$ -pair production. Also, we have used  $x = \frac{1}{2}$  throughout this study.

The plot clearly shows that the cross section for the right-polarized electron beam is greater than that of unpolarized and left-polarized beam. This is expected because, in this scenario, the right selectron is much lighter than the left selectron, and, as a result, the t-channel contribution for neutralino pair production is larger for right than for left-polarized electron beams. It should be remembered that at high energies ( $\sim 500$  GeV) the t-channel contribution dominates over the s-channel one. Moreover, the NLSP is dominated by the Bino-component over most of the parameter space.

It has been shown [19] that the channel  $\tilde{\chi}_1^0 \rightarrow Z\tilde{G}$  can provide a substantial contribution (up to about 23%) to the decay of  $\tilde{\chi}_1^0$ . We have taken this into account in our present calculation by multiplying the results with the appropriate branching fractions.

On the other hand, the same two-photon signal can come from the MSSM scenario when pair-produced  $\tilde{\chi}_2^0$ 's decay radiatively into a photon and an LSP (which is  $\tilde{\chi}_1^0$ ). The branching ratio (BR) of this decay can be as large as of the order of 0.9 if one assumes that  $M_2$  and  $M_1$ , the  $SU(2)$  and  $U(1)$  gaugino masses, respectively, are free parameters [13]. This is

tantamount to at least a partial relaxation of gaugino mass unification at a high-energy scale, but is nonetheless a feasible scenario in a model-independent analysis. It has been shown that in order to have a large BR of this radiative decay, one needs in general  $\mu < 0$ ,  $\tan\beta \geq 1$ . Further, regions where  $M_1 \simeq M_2$  and  $\tan\beta$  is not much larger than 1 are favored. Whenever  $\tilde{\chi}_1^0$  ( $\tilde{\chi}_2^0$ ) is gaugino dominated and  $\tilde{\chi}_2^0$  ( $\tilde{\chi}_1^0$ ) is mainly a Higgsino, the tree-level decay widths of  $\tilde{\chi}_2^0$  get suppressed and the radiative decay  $\tilde{\chi}_2^0 \rightarrow \tilde{\chi}_1^0 \gamma$  is enhanced. This is termed as dynamical enhancement and is discussed in great detail in Ref.[13]. The other source of large BR comes into play when  $(m_{\tilde{\chi}_2^0} - m_{\tilde{\chi}_1^0}) \sim 10$  GeV and  $m_{\tilde{\chi}_2^0, \tilde{\chi}_1^0} \approx M_Z$ , causing a strong phase-space suppression of the three-body decays. This is called kinematical enhancement.

Taking into account all these effects, we see that the cross section for the  $\gamma\gamma + \not{E}$  signal can be comparable to that coming from the GMSB scenario over a large region of the MSSM parameter space. Tables 1 and 2 show these cross sections for unpolarized as well as left- and right- polarized electron beam. In these tables, we have chosen some representative points in the  $(M_1, M_2)$  parameter space where the branching ratio of the radiative decay  $\tilde{\chi}_2^0 \rightarrow \tilde{\chi}_1^0 \gamma$  is large and the  $\gamma\gamma + \not{E}$  cross section is high enough to compare with the GMSB signals shown in Fig. 1. This feature is reflected in the neighborhoods of all of these representative points, although the functional dependence on  $M_1$  and  $M_2$  is rather complicated. The same set of cuts as those applied in Fig. 1 are present here also. We have taken all the slepton masses to be degenerate and equal to 120 GeV (Table 1) and 1 TeV (Table 2). Here we have shown results that are consistent with the limits on various superparticle masses from the LEP experiments upto  $\sqrt{s} = 172$  GeV [20]. It should be borne in mind, however, that such limits are based on the assumption of gaugino mass unification and are liable to relaxation once that assumption is withdrawn.

As is evident from these tables, the unpolarized MSSM signal can often pass off as the signal of GMSB. This is especially true in regions close to the kinematic limit of  $\tilde{\chi}_1^0$ -pair

production in GMSB or in general in cases where the predicted GMSB signal rate is on the lower side. As a first solution to the problem, we study the signals in both scenarios with polarized electron beams. We have already seen that the GMSB signals are jacked up by the choice of right polarisation. In parallel, the MSSM signals in a large number of cases are larger with left-handed electron. This happens whenever  $\tilde{\chi}_2^0$  is dominated by Wino, i.e., the  $SU(2)$  gaugino component. The number of cases with the reverse effect ( $\tilde{\chi}_2^0$  is dominated by the Bino component) is relatively fewer but still nonvanishing. There are some other regions in the parameter space where this statement is no longer true, i.e.,  $\tilde{\chi}_2^0$  is dominated by the Wino component but still  $A^{\gamma\gamma}$  (see, Eq. (7) below) is negative. This happens because in those cases the s-channel contribution becomes important (sleptons masses being very high), and the cross sections are crucially controlled by s-t and s-u interference, where the signs of the mixing factors play a significant role.

Thus, if one defines  $\sigma_{L(R)}^{\gamma\gamma}$  as the cross section for  $e^+e^- \rightarrow \gamma\gamma + \cancel{E}$  with a left(right)-polarized electron, then, if an asymmetry parameter is defined as [9]

$$A^{\gamma\gamma} = \frac{\sigma_L^{\gamma\gamma} - \sigma_R^{\gamma\gamma}}{\sigma_L^{\gamma\gamma} + \sigma_R^{\gamma\gamma}}, \quad (7)$$

the magnitude as well as the sign of  $A^{\gamma\gamma}$  is a clear measure of the sensitivity of the signal to electron polarization. This asymmetry is also tabulated in Tables 1 and 2. The corresponding asymmetry in GMSB is plotted in Fig. 2, which is negative everywhere. So, if  $A^{\gamma\gamma}$  is positive then it comes clearly from MSSM scenario. On the other hand, if  $A^{\gamma\gamma}$  is negative then it is not possible to tell whether the signal comes from GMSB or from MSSM.

We, therefore, are led to the conclusion that polarized beams do not solve the problem completely, and we are forced to devise some other method of separating the two scenarios. One rather elegant way is to see the combined energy distributions  $\frac{d\sigma}{d(E_{\gamma_1} + E_{\gamma_2})}$  of the two emitted photons in those particular cases where  $A^{\gamma\gamma}$  is negative. (Such distributions have

earlier been used [21] to eliminate SM backgrounds.) These energy distributions are plotted in Fig. 3 for unpolarized electron beam. In the case of GMSB, this energy distribution is peaked at a point  $\sim 250$  GeV ( $\frac{\sqrt{s}}{2}$ ) and wider in comparison to the MSSM case, where it is sharply peaked at a point much lower than 250 GeV. These behaviors can be explained in the following manner. In the GMSB case,  $\tilde{\chi}_1^0$  decays into two massless particles. So, the sum of the two photon energies must be peaked at about a point  $\frac{\sqrt{s}}{2}$  which is the missing energy carried by the two  $\tilde{G}$ 's. In the case of MSSM,  $\tilde{\chi}_2^0$  decays into a heavy  $\tilde{\chi}_1^0$  (whose mass is close to that of  $\tilde{\chi}_2^0$ ) and a soft photon. The combined photon energy in this case will be peaked at a point much lower than 250 GeV. The distributions in the two cases have been plotted for comparable values of the total cross section. The spread in the energy distribution mainly depends on the product of the velocity of the decaying particle and the energy of the photon, both measured in the laboratory frame. This feature is reflected in Fig. 3. Thus by looking at the combined energy distributions of the two photons one can readily tell whether the signal comes from GMSB or from the conventional SUSY scenario.

## 4 Pair-production of $\tilde{\chi}_2^0$

In the last section, we have seen that the  $\gamma\gamma + \not{E}$  signal can as well come from MSSM, and that careful analysis is required if one really wants to distinguish between the two pictures through the observation of such events. On the other hand, one can study other possible signals of GMSB and try to analyse whether there are sources which can mimic these. One such signal is  $e^+e^- \rightarrow \tilde{e}_R\tilde{e}_R^* \rightarrow l^+l^-\gamma\gamma + \not{E}$  via a  $\tilde{\chi}_1^0$  which is the NLSP. This process has already been studied in several works [22]. The same signal can also come from MSSM through the cascade decays of a pair of sleptons. It can be large enough in the regions of the parameter space where radiative decay of  $\tilde{\chi}_2^0$  is dominant. In GMSB, the contribution

comes mainly from a right-polarized electron beam via the production of right sleptons, giving rise to a negative asymmetry similar to the one defined in the last section. In the MSSM scenario too, the contributions from right sleptons can be greater than those from left sleptons when  $\tilde{\chi}_2^0$  is dominated by the Bino component and  $\tilde{\chi}_1^0$  is mainly a Higgsino. Here also the asymmetry parameter will be negative. Thus there is a possibility that the above signal also can fake GMSB.

In view of the above, it is desirable to explore further tests of GMSB which are unlikely to be faked by an MSSM scenario. Here we give a brief account of some such signals arising from pair-produced  $\tilde{\chi}_2^0$  in an  $e^+e^-$  collider with  $\sqrt{s} = 500$  GeV. We list below the processes under study, which are governed by the decays of  $\tilde{\chi}_2^0$  [23], cascading into a  $\tilde{\chi}_1^0$  which subsequently goes to a photon and a gravitino:

$$1. \ e^+e^- \rightarrow \tilde{\chi}_2^0\tilde{\chi}_2^0 \rightarrow l^+l^-l^+l^-\gamma\gamma + \cancel{E},$$

$$2. \ e^+e^- \rightarrow \tilde{\chi}_2^0\tilde{\chi}_2^0 \rightarrow l^+l^-jj \ \gamma\gamma + \cancel{E},$$

$$3. \ e^+e^- \rightarrow \tilde{\chi}_2^0\tilde{\chi}_2^0 \rightarrow jj \ \gamma\gamma + \cancel{E}.$$

The intermediate states for the process (1) can be either  $\tilde{\chi}_2^0 \rightarrow \tilde{l}^-\tilde{l}^+(\tilde{l}'-\tilde{l}'^+)$ ,  $\tilde{l}^-(\tilde{l}'-) \rightarrow \tilde{\chi}_1^0l^-(l'^-)$ ,  $\tilde{\chi}_1^0 \rightarrow \gamma\tilde{G}$  or  $\tilde{\chi}_2^0 \rightarrow \tilde{\chi}_1^0Z$ ,  $Z \rightarrow l^+l^-(l^+l^-)$ ,  $\tilde{\chi}_1^0 \rightarrow \gamma\tilde{G}$ . For process (2) they are  $\tilde{\chi}_2^0 \rightarrow \tilde{l}^-\tilde{l}^+$ ,  $\tilde{l}^- \rightarrow \tilde{\chi}_1^0l^-$  and  $\tilde{\chi}_2^0 \rightarrow \tilde{\chi}_1^0Z$ ,  $Z \rightarrow q\bar{q}$ . In case of process (3) they can be  $\tilde{\chi}_2^0 \rightarrow \tilde{\chi}_1^0Z$ ,  $Z \rightarrow \nu\bar{\nu}$  or  $q\bar{q}$ . The cross sections for the three processes have been plotted as functions of  $\Lambda$  in Figs. 4 and 5, for two different combinations of other parameters. Here we have performed a parton level Monte Carlo calculation, setting the criterion for jet merging as  $\Delta R \geq 0.7$ , where  $(\Delta R)^2 = (\Delta\eta)^2 + (\Delta\phi)^2$ ,  $\eta$  and  $\phi$  being pseudorapidity and azimuthal angle, respectively. We have employed a cut of 15 GeV on jet energy and an angular cut  $10^0 < \theta_j < 170^0$ . For the observation of the two emitted photons, a minimum energy cut of 10 GeV and an angular cut  $10^0 < \theta_\gamma < 170^0$  have been used. A similar angular cut on the

emitted leptons has been applied (the last-mentioned cut does not affect the cross sections in a significant manner). The standard model backgrounds for all the signals are rather small [24].

In Fig. 4, we see that channel (3) dominates over the others for higher values of  $\Lambda$  due to the production of real Z. Conversely, channel (1) is more important for lower values of  $\Lambda$ , when only real (right)sleptons are produced. If real Z's are produced at all in such cases, they are kinematically suppressed. In Fig. 5, the cross sections are quite high ( $\sim 0.1\text{pb}$ ) for channel (1) compared to the other channels. In this case,  $\tilde{\chi}_2^0$  is mainly a gaugino with a high production rate, decaying into real sleptons.

The possible sources of confusion with MSSM are  $\tilde{\chi}_3^0\tilde{\chi}_3^0$  or  $\tilde{\chi}_2^0\tilde{\chi}_3^0$  pairs. The subsequent decay of  $\tilde{\chi}_3^0$  via the channel  $\tilde{\chi}_3^0 \rightarrow \tilde{\chi}_2^0 Z$  or  $\tilde{\chi}_3^0 \rightarrow f\tilde{f}, \tilde{f} \rightarrow \tilde{\chi}_2^0 f$  and then the radiative decay of  $\tilde{\chi}_2^0$  into a photon and a  $\tilde{\chi}_1^0$  can give rise to the signals mentioned above. These backgrounds are not very serious due to the following qualitative argument: the decay  $\tilde{\chi}_3^0 \rightarrow \tilde{\chi}_2^0 Z$  will be suppressed if  $\tilde{\chi}_3^0$  and  $\tilde{\chi}_2^0$  are not both dominated by the same Higgsino component. Also, there will be a kinematical suppression for this decay. Again, if  $\tilde{\chi}_3^0$  is dominated by the Higgsino component then the production of  $\tilde{\chi}_3^0$  pair will be very low. The same line of reasoning goes for the  $\tilde{\chi}_3^0\tilde{\chi}_2^0$  pair production and their subsequent decays. Also, the cascade decay of  $\tilde{\chi}_3^0$  via sfermion channel is unlikely to produce signals of appreciable magnitudes, unless all of the three lightest neutralinos have sizable gaugino components.

For example, the  $jj \gamma\gamma + \cancel{E}$  signal can come from the following process:

$$e^+e^- \rightarrow \tilde{\chi}_2^0\tilde{\chi}_3^0 \rightarrow jj \gamma\gamma + \cancel{E},$$

where, the intermediate states are  $\tilde{\chi}_3^0 \rightarrow \chi_2^0 Z$ ,  $Z \rightarrow q\bar{q}$ , and  $\tilde{\chi}_2^0 \rightarrow \tilde{\chi}_1^0 \gamma$ . The cross section for this signal can be at most 0.6-0.7 fb using the same set of cuts which were earlier used in identifying the GMSB signal. The cross-sections for the other processes are always smaller

than this one. Thus we see that the signals coming from the pair-production of  $\tilde{\chi}_2^0$  in GMSB scenario is always large compared to its MSSM counterpart. This definitely happens for  $\Lambda \leq 85$  TeV, where signals with rates on the order of 1 fb and much above are predicted.

## 5 Summary and Conclusions

We have considered the effect of the dominant radiative decay of second lightest neutralino ( $\tilde{\chi}_2^0$ ) in MSSM, assuming partial relaxation of gaugino mass unification at a high-energy scale. It has been shown that this decay may give rise to signals of the type  $\gamma\gamma + \cancel{E}$  in an  $e^+e^-$  collider with  $\sqrt{s} = 500$  GeV. This in turn can fake the GMSB scenario where the same signal is supposed to come from the decay of the lightest neutralino ( $\tilde{\chi}_1^0$ ) into a photon and a gravitino. Our analysis shows that for some region in the MSSM parameter space, this signal is comparable to that coming from GMSB. This is particularly true when the mass of  $\tilde{\chi}_1^0$  in the GMSB scenario is  $\sim 200$  GeV or more, which marks the region beyond which  $\tilde{\chi}_1^0$ -pair production is kinematically more and more suppressed.

The above observations can be generalized to the rather interesting conclusion that the signals associated with the  $n$ th lightest neutralino in a GMSB scenario have always got the chance of being faked by the  $(n+1)$ th lightest neutralino of MSSM. Careful analysis is therefore required to distinguish the two possibilities.

In distinguishing between the two scenarios, we see that the idea of polarization asymmetry is an useful tool. This is actually a measure of sensitivity of the signal to electron polarization. This idea is helpful in separating the two SUSY breaking schemes over a wide region of the MSSM parameter space. Also, one can use the combined energy distributions of the emitted photons for unpolarized electron beam for a clear distinction between the two scenarios, particularly when the polarization asymmetry is of similar nature for both of

them.

In addition we have also studied the signals coming from the next-to-lightest neutralino pairs in GMSB. The signals are considerably free from standard model backgrounds, and contributions from MSSM are generally suppressed. We conclude that such signals can also be useful for the confirmation of GMSB in the parameter range upto  $\Lambda \approx 85$  TeV.

## Acknowledgments

We thank Anirban Kundu for useful discussions. SR wishes to acknowledge the hospitality of the theory group, Saha Institute of Nuclear Physics, Calcutta, where part of this work was done.

## References

- [1] For reviews, see, e.g., H.P. Nilles, Phys. Rep. **110**, 1 (1984); H.E. Haber and G.L. Kane, Phys. Rep. **117**, 75 (1985). For a recent overview, see, e.g., G.L. Kane, hep-ph/9709318.
- [2] M. Dine, W. Fischler, and M. Srednicki, Nucl. Phys. **B189**, 575 (1981); S. Dimopoulos and S. Raby, Nucl. Phys. **B192**, 353 (1981), Nucl. Phys. **B219**, 479 (1983); M. Dine and W. Fischler, Phys. Lett. **110B**, 227 (1982); M. Dine and M. Srednicki, Nucl. Phys. **B202**, 238 (1982); C. Nappi and B. Ovrut, Phys. Lett. **113B**, 175 (1982); M. Dine and W. Fischler, Nucl. Phys. **B204**, 346 (1982); L. Alvarez-Gaumé, M. Claudson and M. B. Wise, Nucl. Phys. **B207**, 96 (1982).
- [3] M. Dine and A.E. Nelson, Phys. Rev. **D48**, 1277 (1993); M. Dine, A.E. Nelson, and Y. Shirman, Phys. Rev. **D51**, 1362 (1995); M. Dine, A.E. Nelson, Y. Nir, and Y. Shirman, Phys. Rev. **D53**, 2658 (1996); G. Dvali, G.F. Giudice, and A. Pomarol, Nucl. Phys. **B478**, 31 (1996).
- [4] S. Dimopoulos and G.F. Giudice, Phys. Lett. **B393**, 72 (1997); G. Dvali and M. Shifman, Phys. Lett. **B399**, 60 (1997); T. Hotta, K.-I. Izawa, and T. Yanagida, Phys. Rev. **D55**, 415 (1997); S.P. Martin, Phys. Rev. **D55**, 3177 (1997); L. Randall, Nucl. Phys. **B495**, 37 (1997).
- [5] S. Borgani, A. Masiero, and M. Yamaguchi, Phys. Lett. **B386**, 189 (1996); A. Riotto, O. Törnkvist and R.N. Mohapatra, Phys. Lett. **B388**, 599 (1996); A. de Gouvêa, T. Moroi, and H. Murayama, Phys. Rev. **D56**, 1281 (1997); N. Arkani-Hamed, J. March-Russel, and H. Murayama, Nucl. Phys. **B509**, 3 (1998); S. Raby, Phys. Rev. **D56**, 2852 (1997); F. Borzumati, hep-ph/9702307.

[6] E. Poppitz and S. Trivedi, Phys. Rev. D**55**, 5508 (1997); N. Haba, N. Maru, and T. Matsuoka, Nucl. Phys. B**497**, 31 (1997), Phys. Rev. D**56**, 4207(1997); Y. Shadmi, Phys. Lett. B**405**, 99(1997); K.-I. Izawa, Prog. Theor. Phys. **95**, 443(1997); H. Murayama, Phys. Rev. Lett. **79**, 18 (1997); S. Dimopoulos, G. Dvali, and R. Rattazzi, Phys. Lett. B**413**, 336(1997); T. Han and R. Hempfling, *ibid.* 415, 161(1997); G. Dvali and A. Pomarol, hep-ph/9708364.

[7] D. Stump, M. Wiest, and C.-P. Yuan, Phys. Rev. D**54**, 1936 (1996); S. Dimopoulos, M. Dine, S. Raby, and S. Thomas, Phys. Rev. Lett. **76**, 3494 (1996); S. Dimopoulos, S. Thomas, and J. D. Wells, Phys. Rev. D**54**, 3283 (1996); S. Ambrosanio, G.L. Kane, G.D. Kribs, S.P. Martin, and S. Mrenna, Phys. Rev. Lett. **76**, 3498 (1996), Phys. Rev. D**54**, 5395 (1996); K.S. Babu, C. Kolda, and F. Wilczek, Phys. Rev. Lett. **77**, 3070 (1996); R. Rattazzi and U. Sarid, Nucl. Phys. B**501**, 297(1997).

[8] H. Baer, M. Brhlik, C. Chen, and X. Tata, Phys. Rev. D**55**, 4463 (1997); J.L. Lopez, D.V. Nanopoulos, and A. Zichichi, Phys. Rev. Lett. **77**, 5168 (1996), Phys. Rev. D**55**, 5813 (1997); D.A. Dicus, B. Dutta, and S. Nandi, Phys. Rev. Lett. **78**, 3055 (1997).

[9] A. Ghosal, A. Kundu, and B. Mukhopadhyaya, Phys. Rev. D**56**, 504 (1997).

[10] S. Ambrosanio, G. Kribs, and S.P. Martin, Phys. Rev. D**56**, 1761 (1997); D.A. Dicus, B. Dutta, and S. Nandi, *ibid.* **56**, 5748(1997); C.H. Chen and J.F. Gunion, hep-ph/9707302; J. Kim, J.L. Lopez, D.V. Nanopoulos, R. Rangarajan, and A. Zichichi, Phys. Rev. D**57**, 373(1998); E. Gabrielli and U. Sarid, Phys. Rev. Lett. **79**, 4752(1997); Y. Nomura and K. Tobe, hep-ph/9708377.

[11] A. Datta, A. Datta, A. Kundu, B. Mukhopadhyaya, and S. Roy, Phys. Lett. B**416**, 117(1998).

- [12] See, e.g., Stump *et al.* [7]; Ambrosanio *et al.* [7]; Ambrosanio *et al.* [10].
- [13] S. Ambrosanio and B. Mele, Phys. Rev. D**55**, 1399 (1997); **56**, 3157(E) (1997).
- [14] J. Bagger, K. Matchev, D. Pierce, and R.-J Zhang, Phys. Rev. Lett. **78**, 1002 (1997); **78**, 2497(E) (1997); Phys. Rev. D**55**, 3188 (1997); S. Dimopoulos, S. Thomas and J.D. Wells, Nucl. Phys. **B488**, 39 (1997).
- [15] See, e.g., Dimopoulos *et al.* [7]; Baer *et al.* [8].
- [16] See, e.g., Ambrosanio *et al.* [7, 10].
- [17] See, e.g., Stump *et al.* [7]; Ghosal *et al.* [9].
- [18] D $\emptyset$  Collaboration, B. Abbott *et al.* Phys. Rev. Lett. **80**, 442(1998).
- [19] See, e.g., Datta *et al.* [11].
- [20] The OPAL Collaboration, K. Ackerstaff *et al.*, hep-ex/9708018.
- [21] See, Stump *et al.* [7].
- [22] See, e.g., Ambrosanio *et al.* [7, 10].
- [23] A. Bartl, H. Fraas, and W. Majerotto, Nucl. Phys. **B278**, 1 (1986).
- [24] For the cuts used in some other studies in linear  $e^+e^-$  colliders, see, for example, R. Rückl, R. Settles, and H. Spiesberger, hep-ph/9709315.

$M_1$ (GeV)	$M_2$ (GeV)	$\sigma_{tot}^{\gamma\gamma}$ (fb)	$\sigma_L^{\gamma\gamma}$ (fb)	$\sigma_R^{\gamma\gamma}$ (fb)	$A^{\gamma\gamma}$
70	60	3.10	2.68	3.53	-0.13
80	60	2.25	1.12	3.38	-0.50
90	60	1.76	0.72	2.80	-0.59
90	120	3.20	2.02	4.38	-0.36
100	90	74.64	89.10	60.18	0.19
100	100	131.9	131.87	131.99	-0.0004
100	130	8.85	5.00	12.70	-0.43
110	100	68.75	85.00	52.50	0.23
110	120	74.90	60.00	89.75	-0.19
120	80	43.80	80.25	7.33	0.83
120	90	65.90	112.75	19.00	0.71
140	70	21.49	42.75	0.23	0.99
140	90	10.00	19.40	0.58	0.94
150	70	21.92	43.75	0.09	0.99
150	90	9.36	18.50	0.23	0.97

**Table 1**

Sample values of the cross-sections for  $e^+e^- \rightarrow \gamma\gamma + E$ , and the asymmetry parameter in MSSM, for  $\mu = -M_Z$ ,  $\tan\beta = 1.2$ ,  $m_{\tilde{e}} = 120$  GeV,  $m_{\tilde{q}} = 300$  GeV.  $\sqrt{s} = 500$  GeV.

$M_1$ (GeV)	$M_2$ (GeV)	$\sigma_{tot}^{\gamma\gamma}$ (fb)	$\sigma_L^{\gamma\gamma}$ (fb)	$\sigma_R^{\gamma\gamma}$ (fb)	$A^{\gamma\gamma}$
50	50	15.10	17.40	12.80	0.15
50	60	3.14	3.72	2.55	0.18
60	60	8.50	9.80	7.20	0.15
70	50	2.73	2.80	2.65	0.02
70	70	4.10	4.70	3.50	0.14
70	80	2.49	2.95	2.03	0.18
100	110	2.39	1.94	2.83	-0.18
100	120	2.47	1.62	3.32	-0.34
110	90	2.41	3.60	1.21	0.49
110	100	3.34	4.13	2.55	0.23
110	120	3.67	2.91	4.43	-0.20
120	110	4.01	5.06	2.97	0.26
160	60	1.58	0.81	2.35	-0.48
170	60	1.74	0.89	2.59	-0.48
180	60	1.91	1.01	2.81	-0.47

**Table 2**

Sample values of the cross-sections for  $e^+e^- \rightarrow \gamma\gamma + E$ , and the asymmetry parameter in MSSM, for  $\mu = -M_Z$ ,  $\tan\beta = 1.2$ ,  $m_{\tilde{e}} = 1000$  GeV,  $m_{\tilde{q}} = 1000$  GeV.  $\sqrt{s} = 500$  GeV.

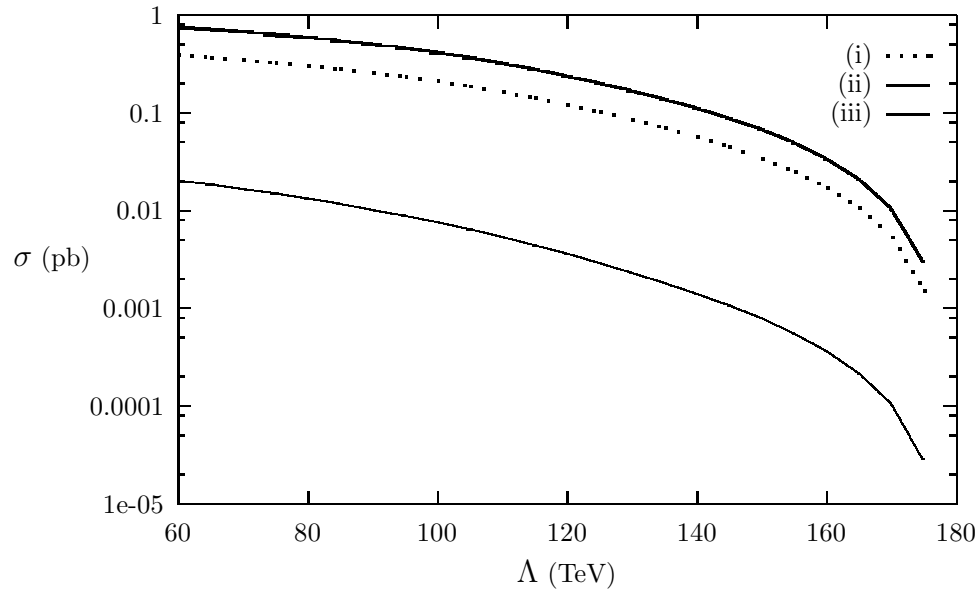


**Figure 1**

Cross-section for  $e^+e^- \rightarrow \gamma\gamma + \cancel{E}$  as a function of  $\Lambda$  ( $\sqrt{s} = 500$  GeV). The three lines corresponds to (i) unpolarized, (ii) left-polarized, and (iii) right-polarized electron beam. Here  $\mu = 900$  GeV,  $\tan\beta = 2$ ,  $\frac{M}{\Lambda} = 2$ . The cuts used here are already stated in the text.

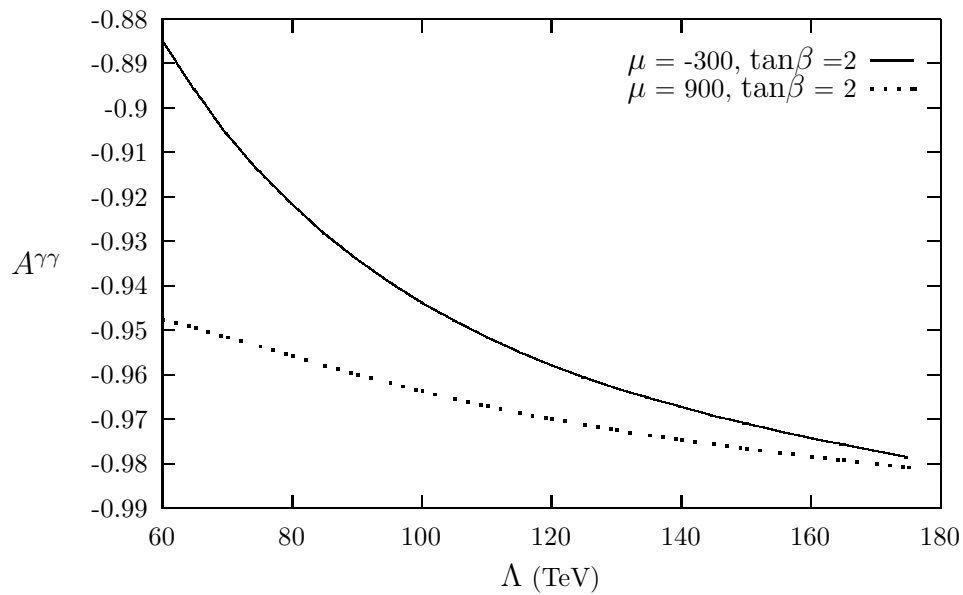


**Figure 2**

Asymmetry parameter  $A^{\gamma\gamma}$  is plotted as a function of  $\Lambda$  for two different sets of  $\mu$  and  $\tan\beta$ .  
 $\frac{M}{\Lambda} = 2$ .

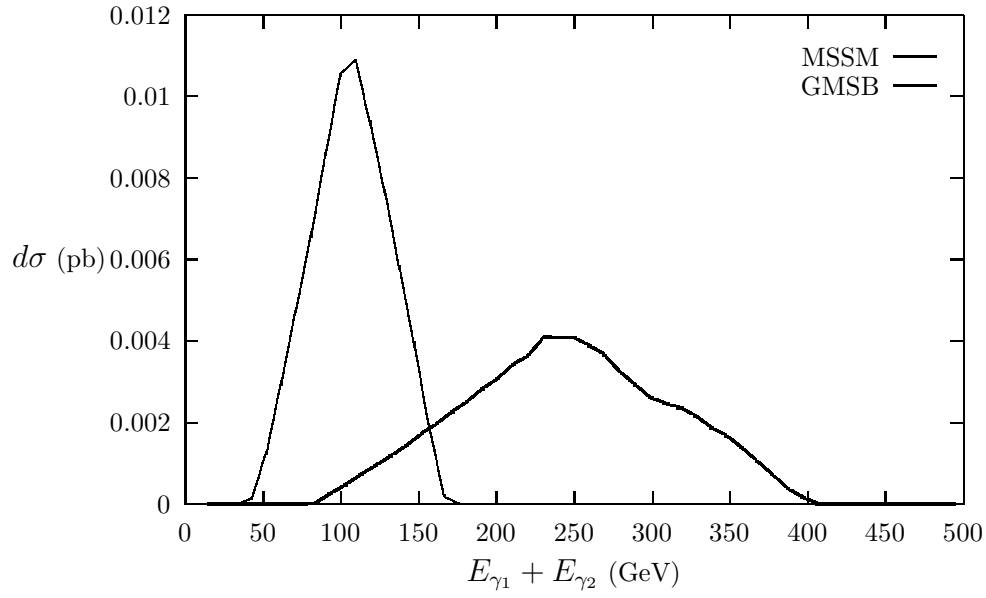


**Figure 3**

Total energy distributions of the emitted photons with the cuts as stated in the text. For GMSB,  $\mu = 900$  GeV,  $\tan\beta = 2$ ,  $M = 270000$  GeV and  $\frac{M}{\Lambda} = 2$ . For MSSM,  $\mu = -M_Z$ ,  $\tan\beta = 1.2$ ,  $m_{\tilde{e}} = 120$  GeV,  $m_{\tilde{q}} = 300$  GeV,  $M_2 = 120$  GeV, and  $M_1 = 110$  GeV.

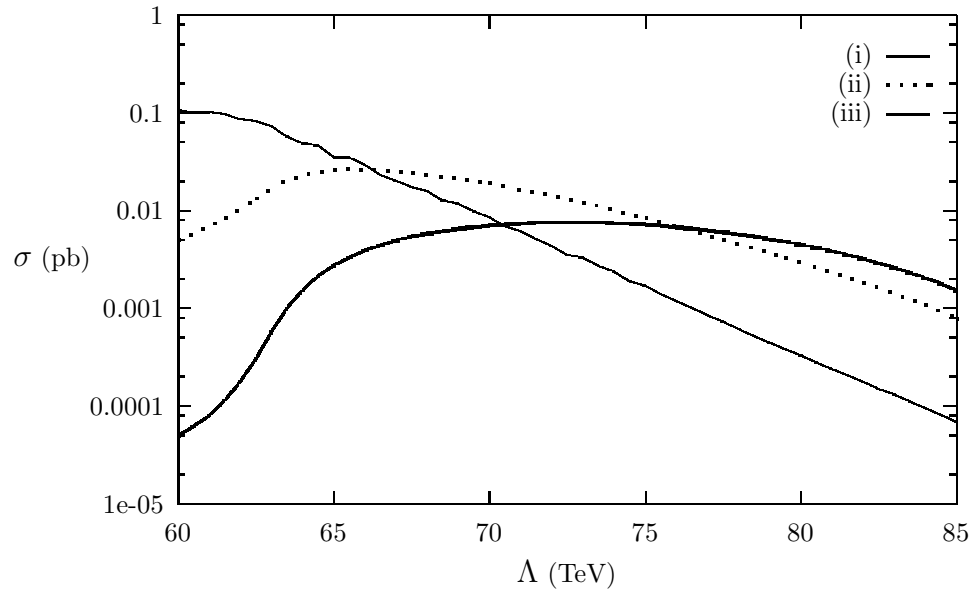


**Figure 4**

Cross-sections for (i)  $e^+e^- \rightarrow l^+l^-l'^+l'^-\gamma\gamma + \cancel{E}$ , (ii)  $e^+e^- \rightarrow jj \ l^+l^-\gamma\gamma + \cancel{E}$ , and (iii)  $e^+e^- \rightarrow jj \ \gamma\gamma + \cancel{E}$  as functions of  $\Lambda$ , for  $\sqrt{s} = 500$  GeV. Here  $\mu = -300$ ,  $\tan\beta = 2$ ,  $\frac{M}{\Lambda} = 2$ .

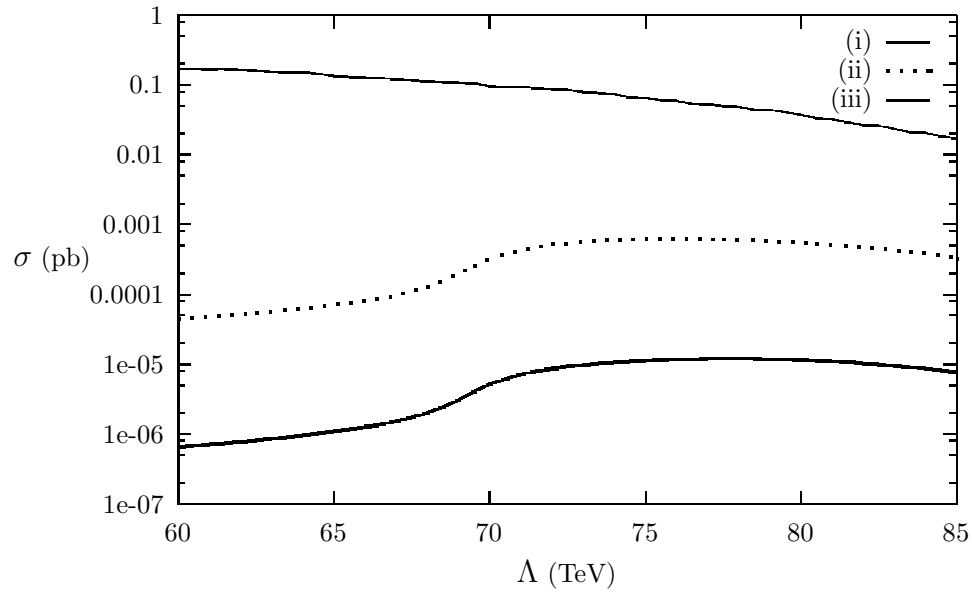


**Figure 5**

Cross-sections for (i)  $e^+e^- \rightarrow l^+l^-l'^+l'^-\gamma\gamma + \not{E}$ , (ii)  $e^+e^- \rightarrow jj \ l^+l^-\gamma\gamma + \not{E}$ , and (iii)  $e^+e^- \rightarrow jj \ \gamma\gamma + \not{E}$  as functions of  $\Lambda$ , for  $\sqrt{s} = 500$  GeV. Here  $\mu = 900$ ,  $\tan\beta = 2$ ,  $\frac{M}{\Lambda} = 2$ .